JOURNAL OF CATALYSIS 154, 335–344 (1995)

Cyclohexene Hydrogenation Catalyzed by MgO-Supported Tetrairidium Clusters

Z. Xu and B. C. Gates[1]

Department of Chemical Engineering and Materials Science, University of California at Davis, Davis, California 95616

Received July 14, 1994; revised February 7, 1995

Tetrairidium clusters supported on MgO powder were prepared by decarbonylation of supported $[HIr_4(CO)_{11}]^-$ by treatment in He followed by H_2 at 300°C. Infrared spectroscopy showed that the CO ligands were fully removed, and extended X-ray absorption fine structure (EXAFS) spectroscopy indicated that the tetrahedral metal frame was retained. Thus the sample is represented as Ir_4/MgO. H_2 chemisorption measurements indicate that the clusters adsorb less H_2 than supported metallic crystallites; the H : Ir ratio was only 0.25. Temperature-programmed desorption indicated strong interactions between adsorbed hydrogen and iridium, represented by the major desorption peak at about 440°C. Ir_4/MgO was tested as a catalyst for cyclohexene hydrogenation in the presence of liquid-phase reactants at 25°C and 1 atm. The used catalyst was characterized by EXAFS spectroscopy and found not to have changed significantly during the catalytic reaction. The first-shell Ir–Ir coordination number was 3.3, the same, within experimental error, as that of the MgO-supported $[HIr_4(CO)_{11}]^-$ precursor and the sample formed by its decarbonylation. The turnover frequency was found to be $0.018 \pm 0.006\ s^{-1}$, which is two orders of magnitude less than that of conventional highly dispersed supported metallic catalysts. It is inferred that the small supported clusters are quasi-molecular and catalytically distinct from supported metallic clusters.

INTRODUCTION

Structure sensitivity is one of the central concepts unifying metal catalysis (1, 2). Structure-insensitive reactions proceed at approximately the same turnover frequency (TOF) on different crystal planes of a particular metal and on the surfaces of metallic particles of various sizes. One of the most thoroughly investigated structure-insensitive reactions is cyclohexene hydrogenation, which was investigated by Boudart *et al.* in the presence of liquid-phase reactants and catalysts consisting of metal-oxide-supported particles of Pt (3–6), Pd (7), Rh (8), and Ni (9); metal dispersions ranged from 14 to 100%. The TOF was found to be independent of the metal particle size for particles ≥9 Å in diameter. The TOFs characterizing the reaction catalyzed by platinum crystallites nearly match those of the reaction catalyzed by single-crystal platinum exposing a stepped (223) face (10). Because the reaction has been found to be nearly zero order in cyclohexene, Boudart and Djéga-Mariadassou (2) concluded that the metallic surface was largely covered with alkyl groups and tentatively suggested that the structure insensitivity is a consequence of the fact that the reaction takes place on "metal-alkyl" surfaces where structural features have been "essentially erased."

The supported catalysts referred to above all evidently incorporated metals in particles large enough to be essentially metallic. As metal crystallites or clusters become smaller, a limit is reached at which they are no longer metallic (11). In the limit of a single metal atom on a metal oxide surface (which is presumably almost always present as a cation in a mononuclear metal complex), the concepts of catalysis on metallic surfaces no longer pertain, and TOFs observed in catalysis by such complexes are generally less than those characterizing the same metal in a metallic state (8). It is not yet evident how small metal clusters may become before they are no longer essentially metallic and the concept of structure sensitivity breaks down. Virtually all the data characterizing structure (in)-sensitivity in supported metal catalysis pertain to metal particles with average sizes greater than about 10 Å (2, 8). Supported clusters smaller than these have not yet been well investigated because they are difficult to prepare and characterize.

The goals of the research summarized here were to prepare extremely small and structurally well defined supported metal clusters and to investigate their catalytic activity for cyclohexene hydrogenation. MgO-supported iridium clusters were prepared from an organometallic precursor, $[Ir_4(CO)_{12}]$, to give supported metal clusters with nearly unique nuclearities (numbers of metal atoms), represented as Ir_4/MgO (10). The performance of this

[1] To whom correspondence should be addressed.

0021-9517/95 $12.00

catalyst has been determined in experiments similar to those reported by the Boudart group.

EXPERIMENTAL METHODS

Reagents and Materials

The syntheses and sample transfers were conducted with exclusion of air and moisture on a double-manifold Schlenk vacuum line and in a N_2-purged Braun 150 glovebox. H_2, formed by electrolysis of deionized water in a Balston 75-33 hydrogen generator (specified by the manufacturer to give H_2 with a purity of 99.99999+%), flowed through three traps, one containing 4A zeolite to remove water and others containing Cu_2O and MnO reduced at 400°C to remove O_2. The MnO trap served as an indicator, because trace amounts of O_2 cause a color change from green to dark brown. Tetrahydrofuran (THF) and *n*-hexane solvent (>99%, Fisher) were distilled over sodium benzophenone ketyl and degassed by sparging of dry N_2. Bis(triphenylphosphine)nitrogen(1+) chloride, [PPN][Cl], was dried overnight at 100°C and stored in the drybox. $[Ir_4(CO)_{12}]$ (Strem) was used without purification. A commercial $Pt/\gamma\text{-}Al_2O_3$ catalyst containing 1 wt% Pt was obtained from AESAR (particle size <300 μm); a similar $Pt/\gamma\text{-}Al_2O_3$ sample with a lower metal dispersion was also used.

Partially dehydroxylated MgO was prepared by calcining MgO (MX-65-1 powder, particle size <200 μm, MCB reagents) in flowing O_2 (Matheson Extra Dry Grade) which was heated to 400°C at a rate of approximately 3°C/min. This temperature was held for 2 h, and then the MgO was evacuated at approximately 10^{-3} Torr, held at 400°C for 14 h, cooled under vacuum to room temperature, and stored in the drybox. The MgO had a BET surface area of 75 m^2/g.

Strict precautions were taken in the treatment and storage of cyclohexene because hydroperoxides in this reagent cause deactivation of supported metal catalysts (3). The cyclohexene (>99%, Aldrich) was supplied with a stabilizer to minimize the formation of the explosive hydroperoxides. The reagent was purified by a method similar to that reported (3): A heated 25-cm glass tube containing particles of $\gamma\text{-}Al_2O_3$ was sealed with a septum, through which cyclohexene could be injected by syringe. A side arm with a stopcock was used as a gas inlet. The bottom of the tube was connected to a 50-mL flask for storage of cyclohexene; this also served as a gas outlet. The tube was heated to 400°C at a rate of 10°C/min as He flowed at 60 mL(NTP)/min. This temperature was held for 2 h. After the tube had been cooled to room temperature, the He flow rate was increased to 100 ml(NTP)/min and continued for 30 min. During the He flow, 10 ml of cyclohexene was injected into the tube with an airtight syringe and flowed through the column and into the flask, with the procedure lasting about a day. Just before the start of the catalytic reaction, the cyclohexene was withdrawn with an airtight syringe and injected into the reactor as the He flow continued. The cyclohexene was not stored for more than 3 days.

Sample Preparation

Preparation of MgO-supported $[HIr_4(CO)_{11}]^-$. The procedure for preparing the supported catalyst from $[Ir_4(CO)_{12}]$ and MgO was as follows: 0.072 g of $[Ir_4(CO)_{12}]$ was mixed with 5 g of MgO in a Schlenk flask in the drybox; sufficient $[Ir_4(CO)_{12}]$ was added to give samples containing 1 wt% Ir, assuming complete uptake. After the flask had been removed from the drybox, 30 ml of degassed hexanes was added by cannula. The slurry was stirred at room temperature for 4 h, after which the solution was clear, indicating complete uptake of $[Ir_4(CO)_{12}]$ by the solid. The mixture was evacuated overnight to remove the solvent; the remaining solid was stored in the drybox.

Preparation of Ir_4/MgO *by decarbonylation of MgO-supported* $[HIr_4(CO)_{11}]^-$. The MgO-supported $[HIr_4(CO)_{11}]^-$ was loaded into a glass tube in the drybox and sealed. The tube was brought to 300°C with He flowing through it; the heating rate was 3°C/min. The catalyst was treated in flowing He at 300°C for 2 h and then in flowing H_2 for 2 h. The sample, after cooling to room temperature in flowing H_2 and transfer to the drybox, was light yellow. Infrared spectra were recorded after each sample preparation to confirm that the carbonyl ligands were completely removed by the treatment.

Treatment of $\gamma\text{-}Al_2O_3$*-supported Pt catalyst.* Before the $\gamma\text{-}Al_2O_3$-supported platinum catalyst was used for cyclohexene hydrogenation, it was treated with flowing H_2 as the temperature was raised to 400°C at a rate of 3°C/min and held at 400°C for 2 h. It was then cooled to room temperature in flowing H_2.

Characterization

Extraction of surface species. In the drybox, 0.1 g of the supported sample prepared from MgO and $[Ir_4(CO)_{12}]$ was placed in a 10-ml round-bottom flask and mixed with 0.02 g of [PPN][Cl], an amount sufficient for extraction of all the $[HIr_4(CO)_{11}]^-$. The flask was sealed with a septum and removed from the drybox. THF (5 ml) was transferred to the flask by cannula, and the mixture was stirred for 5 min at room temperature. The solid became white and the solution yellow, indicating that the extraction (by ion exchange) was virtually complete. The solution was removed by syringe and transferred to an air-tight liquid cell for infrared spectroscopy.

Infrared spectroscopy. Transmission infrared spectra were recorded with a Bruker IFS 66v spectrometer with a resolution of 4 cm^{-1}. Solid samples were pressed into thin self-supporting wafers in the drybox and loaded into a controlled-atmosphere cell equipped with NaCl windows. Spectra were measured during gas treatments at various temperatures. Liquid samples were transferred with an air-tight syringe to a 0.1-mm NaCl cell. Each sample was scanned within 2 min. The infrared spectra characterizing each sample were ratioed to the background atmosphere in the spectrometer, and the infrared bands representative of the solvent were subtracted from the spectrum. Each reported spectrum is the average of 64 or more scans.

Infrared spectra were recorded during decarbonylation of supported iridium carbonyl clusters. Each MgO-supported sample containing $[HIr_4(CO)_{11}]^-$ was pressed into a wafer and loaded into an infrared cell in the drybox. The cell was mounted in the spectrometer and the temperature raised at a rate of 3°C/min to 300°C as He flowed over the sample. The sample was held at 300°C for 2 h, H_2 flow was started, and the sample was held under these conditions for 2 h. Spectra were measured during the treatments. Gas flow rates were 60 ml(NTP)/min.

Chemisorption measurements. Chemisorption measurements were performed on an RMX-100 multifunctional catalyst testing and characterization instrument (Advanced Scientific Designs, Inc.). The H_2 formed by electrolysis of water was purified by passage through traps containing Cu_2O and 4A zeolite particles. The catalyst samples (0.2 to 0.4 g) in the drybox were loaded into a quartz tube and connected to the system without exposure to air. The H_2 flow rate was set at 30 ml(NTP)/min. The sample in flowing H_2 was heated to 300°C at a rate of 3°C/min, held at 300°C for 2 h, and evacuated for 30 min at 10^{-6} Torr at the same temperature. After this sample was cooled to room temperature, the first isotherm was measured immediately. After the first set of measurements, the sample was evacuated for 30 min at room temperature, and the procedure was repeated. The amount of chemisorbed hydrogen was obtained by extrapolating the linear high-pressure part of the isotherm to zero pressure and taking the difference between the two isotherms.

CO chemisorption experiments were performed similarly, immediately after the H_2 chemisorption experiments.

Temperature Programmed Desorption (TPD). The TPD of H_2 from the decarbonylated sample formed from MgO-supported $[HIr_4(CO)_{11}]^-$ was investigated with the RMX-100 instrument by direct evacuation of the samples under high vacuum and heating at a rate of 15°C/min to 900°C. Desorbed gases were monitored by mass spectrometry.

Catalytic Reaction

Cyclohexene hydrogenation catalysis was investigated at 1 atm and 25 ± 0.2°C, with the reactor being a 250-ml round-bottom Schlenk flask immersed in a water bath. H_2 flowed continuously through the reactor at rates that were held constant within about ± 1% by a Brooks mass flow controller. The H_2 flowed out of the reactor through an ice-cooled condenser.

The reactor in the drybox was loaded with 40 mg of catalyst, sealed with a double-layer septum, and placed into the water bath. H_2 flowed into the reactor through a syringe needle passing through the septum and extending to the bottom of the flask, purging the reactor for 30 min prior to addition of liquids. *n*-Hexane (100 ml) was distilled and degassed in N_2 for 30 min and transferred into the reactor by cannula. With the H_2 flow rate maintained at 30 ml(NTP)/min, 1.00 ml of cyclohexene was injected into the reactor through an air-tight syringe at time zero; cyclohexene did not flow out of the reactor. Liquid samples (0.2 ml) were withdrawn periodically by syringe and analyzed for the product cyclohexane in a Hewlett-Packard 5890 gas chromatograph equipped with a flame ionization detector and a 30-m × 0.53-mm DB-624 capillary column (J&W Scientific). N_2 was the carrier gas (5 ml/min); the column temperature was 50°C.

Extended X-Ray Absorption Fine Structure (EXAFS) Spectroscopy

A used catalyst sample was prepared as follows for characterization by EXAFS spectroscopy: A sample prepared as described above was tested for the catalytic hydrogenation reaction in the standard way, being kept in operation for 3 h. After removal of the solvent by evacuation at 10^{-3} Torr for 12 h, the sample was transferred to the drybox, sealed in two layers of glass vials, each individually sealed with Parafilm and electrical tape, and placed in a desiccator. The desiccator, filled with dried silica gel, was sealed and evacuated, and the samples were transported to the synchrotron; the EXAFS measurements were made within two days.

EXAFS experiments were performed on beamline X-11A at the National Synchrotron Light Source at Brookhaven National Laboratory. The ring energy was 2.5 Gev and the ring current was 80–220 mA. The X-ray monochromator included a pair of Si(111) crystals. Data were recorded with the sample in a cell that allowed treatment in flowing gases prior to the measurements. The powder samples were pressed into wafers with a C clamp either inside a N_2-filled glovebox or inside a glovebag that was purged with N_2 boiloff gas from a liquid nitrogen cylinder. The amount of sample in a wafer (approximately 150 mg) was calculated to give an absorbance of 2.5 at the Ir L_{III} absorption edge. After the sample had been pressed into a wafer, it was unloaded from the die and placed in the

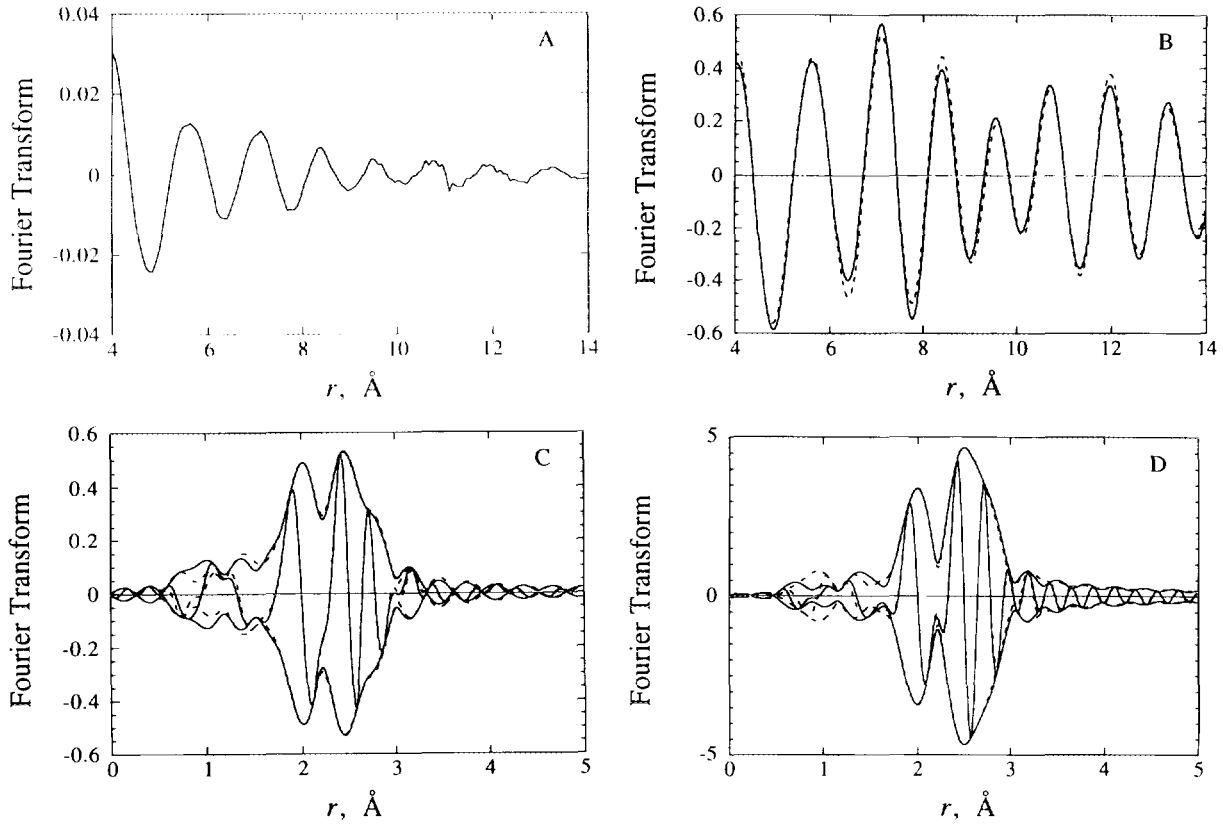

FIG. 1. Results of EXAFS analysis obtained with the best calculated coordination parameters for the used cyclohexene hydrogenation catalyst represented as Ir_4/MgO: A, raw EXAFS data; B, experimental EXAFS (solid line) and sum of the calculated Ir–Ir + Ir–$O_{support}$ (Ir–O_s + Ir–O_l) contributions (dashed line); C, imaginary part and magnitude of the Fourier transform (k^1-weighted, Δk = 3.66–13.80 Å^{-1}) of the experimental EXAFS (solid line) and sum of the calculated Ir–Ir + Ir–$O_{support}$ contributions (dashed line); D, imaginary part and magnitude of the Fourier transform (k^3-weighted, Δk = 3.66–13.80 Å^{-1}) of the experimental EXAFS (solid line) and sum of the calculated Ir–Ir + Ir–$O_{support}$ contributions (dashed line); E, residual spectrum illustrating the EXAFS contributions characterizing the metal–metal interaction, the imaginary part and magnitude of the Fourier transform (k^1-weighted, Δk = 3.66–10.00 Å^{-1}) of the raw data minus the calculated Ir–O_s + Ir–O_l EXAFS (solid line) and the calculated Ir–Ir EXAFS (dashed line); F, residual spectrum illustrating the EXAFS contributions characterizing the metal–metal interaction, the imaginary part and magnitude of the Fourier transform (k^3-weighted, Δk = 3.66–10.00 Å^{-1}) of the raw data minus the calculated Ir–O_s + Ir–O_l EXAFS (solid line) and the calculated Ir–Ir EXAFS (dashed line); G, residual spectrum illustrating the EXAFS contributions characterizing the metal–support interaction, imaginary part and magnitude of the Fourier transform (k^3-weighted, Δk = 3.66–10.00 Å^{-1}) of the raw data minus the calculated Ir–O_s + Ir–O_l EXAFS (solid line) and the calculated Ir–Ir EXAFS (dashed line).

EXAFS cell. The cell was then sealed under a positive pressure of N_2, removed from the drybox or glovebag, aligned in the X-ray beam, and cooled to approximately liquid nitrogen temperature. The EXAFS data were recorded in the transmission mode in the region of the Ir L_{III} absorption edge (11215 eV). The monochromator was detuned by 30% to minimize the effects of higher harmonics in the X-ray beam. The sample was scanned twice.

RESULTS

Characterization of Adsorbed and Extracted Species by Infrared Spectroscopy

After the slurry of $[Ir_4(CO)_{12}]$ and MgO in hexanes had been stirred for 1 h, the color of the solid changed from white to light yellow, showing that $[Ir_4(CO)_{12}]$ had been adsorbed. The infrared spectrum of the resultant solid species, after removal of the hexanes, was characterized by ν_{CO} bands at 2047 s, 2007 s, and 1978 sh cm^{-1}. This spectrum is in agreement with that reported by Maloney *et al.* (13), as expected, and different from the spectrum of $[Ir_4(CO)_{12}]$ in THF (2068 vs, 2027 s) (14). Extraction of the surface species with [PPN][Cl] in THF gave a yellow solution characterized by ν_{CO} bands at 2022 s, 2005 sh, 1962 s, 1938 sh, and 1894 m cm^{-1}, similar to the spectrum of $[HIr_4(CO)_{11}]^-$ in THF solution (15) and in good agreement with the spectrum of Maloney *et al.* (13), who similarly extracted $[HIr_4(CO)_{11}]^-$ from the surface of MgO. The results are consistent with the inference (13) that $[Ir_4(CO)_{12}]$ reacted with OH groups of the basic MgO surface, resulting in the formation of $[HIr_4(CO)_{11}]^-$ as the principal species bound to the MgO surface.

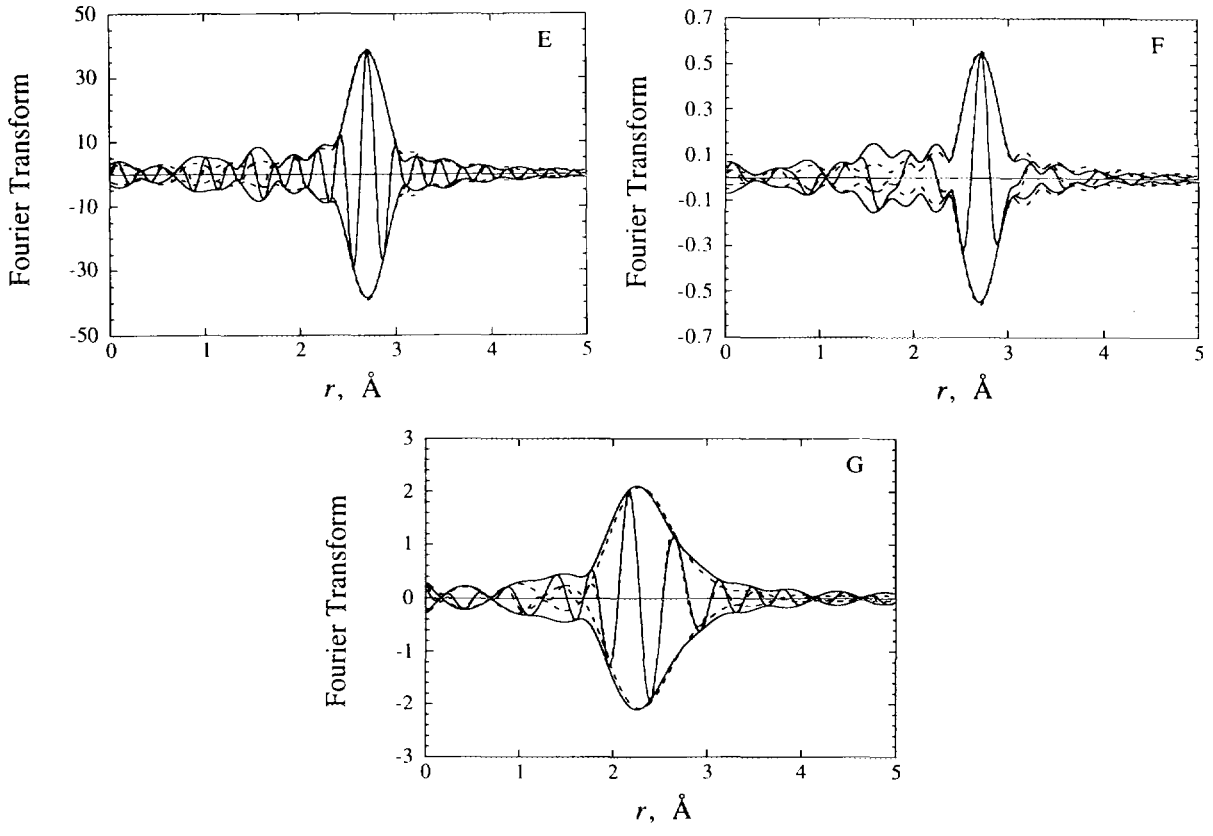

FIG. 1—*Continued*

Decarbonylation of MgO-Supported $[HIr_4(CO)_{11}]^-$

The decarbonylation of the MgO-supported $[HIr_4(CO)_{11}]^-$ was monitored by infrared spectroscopy, with the spectra showing that no carbonyl ligands were left on the surface after treatment in He followed by H_2 at 300°C.

Chemisorption Measurements

The chemisorption data show that the H : Ir ratio representing the sample made by decarbonylation of MgO-supported $[HIr_4(CO)_{11}]^-$ was 0.27 ± 0.03. The CO : Ir value was found to be 0.33 ± 0.04. H_2 chemisorption on the AESAR Pt/Al_2O_3 sample, after heating to 450°C at 3°C/min in flowing of H_2, gave a H : Pt value of 0.84. This result is similar to what has been observed previously for highly dispersed $Pt/\gamma\text{-}Al_2O_3$ samples (16). The other Pt/Al_2O_3 was found to have a dispersion of 0.65.

EXAFS Data and Analysis

The normalized EXAFS function characterizing the used catalyst was obtained from the averaged X-ray absorption spectra by a cubic spline background subtraction and normalized to the height of the absorption edge. The raw EXAFS data characterizing the sample are shown in Fig. 1A. The data show reliable oscillations up to a value of k, the wave vector, of about 13.8 $Å^{-1}$. Oscillations in the intermediate and higher ranges of k ($8 < k < 12$ $Å^{-1}$) indicate the presence of near-neighbor high-Z backscatterers, which are inferred to be iridium atoms.

The EXAFS analysis was done with experimentally determined reference files (Table 1) (17–19). The raw EXAFS data were Fourier transformed with a k^2 weighting and no correction over the useful range ($3.56 < k < 13.8$ $Å^{-1}$). The major contributions were isolated by inverse Fourier transformation in the range $0.63 < r < 3.20$ Å (where r is the distance from the absorber Ir atom) to isolate the major contributions from low-frequency noise and higher-shell contributions. With the Koningsberger difference file technique (20), the Ir–Ir contribution, the largest in the EXAFS spectrum, was estimated by calculating an EXAFS spectrum that agreed as closely as possible with the experimental results in the high-k range ($7.5 < k < 14$ $Å^{-1}$); the metal-support contributions in this region are small because the backscatterers in the support have low atomic weights. An EXAFS function calculated with the first-guess parameters was then subtracted from the data, with the residual spectrum being expected to represent the $Ir–O_{support}$ interactions. The difference file was estimated with two Ir–O contributions, as both short (21)

TABLE 1

EXAFS Results Characterizing the MgO-Supported Iridium Clusters after Use as a Catalyst for Cyclohexene Hydrogenation[a,b]

Shell	N	R (Å)	$\Delta\sigma^2$ (Å^2)	ΔE_0 (eV)	EXAFS reference
Ir–Ir	3.3	2.71	0.00269	−0.80	Pt–Pt
Ir–$O_{support}$:					
Ir–O_s	1.8	2.18	0.0012	−3.95	Pt–O
Ir–O_l	1.7	2.69	0.0048	−7.42	Pt–O

[a] N is the coordination number, R is the average absorber–backscatterer distance, $\Delta\sigma^2$ is the Debye–Waller factor, and ΔE_0 is the inner potential correction. The subscripts l and s refer to long and short, respectively

[b] Estimated precision: N, ±20% (Ir–O_l + Ir–O_s, ±30%); R, ±2% (Ir–Ir, ±1%); $\Delta\sigma^2$, ±30%; ΔE_0, ±10%.

and long (21) metal–support oxygen distances have been observed. As a first approximation, only four free parameters were estimated ($\Delta\sigma^2$, the Debye–Waller factor, and ΔE_0, the inner potential correction, were each set equal to 0) to shorten the computational time.

The first-guess Ir–Ir and Ir–$O_{support}$ contributions were then added and compared with the raw data in r space, and the fit was not yet satisfactory. Then the Ir–Ir contribution was subtracted from the data and more accurate parameters for the contributions of the metal–support interface were determined by fitting the metal–support contributions to the residual spectrum with all eight parameters; the initial guesses for parameter estimation were determined by adjusting the coordination parameters to give the best agreement with the residual spectrum, both in k space and in r space, with both k^1 and k^3 weighting. The iteration was continued until the fit was good.

The Ir–Ir and two Ir–$O_{support}$ contributions were then added, representing the overall fit of the data. To show the goodness of the fit for both the high-Z (Ir) and low-Z (O) contributions, the raw data are compared with the fit, both in k space (with k^2 weighting) and in r space (with both k^1 and k^3 weighting) in Figs. 1B–1D. The agreement is good. The Ir–Ir contribution is shown in the difference file of Fig. 1F, and the Ir–$O_{support}$ contribution is shown in the difference file of Fig. 1G. The structure parameters are summarized in Table 1. The first-shell Ir–Ir coordination number was found to be 3.3, the Ir–O_s coordination number was 1.8, and the Ir–O_l coordination number was 1.7, where the subscripts s and l refer to short and long, respectively.

The number of parameters used to fit the data in this main-shell analysis is 12; the statistically justified number is approximately 15, estimated from the Nyquist theorem (22), $n = (2\,\Delta k\,\Delta r/\pi) + 1$, where Δk and Δr, respectively, are the k and r ranges used in the forward and inverse Fourier transforms (Δk = 10.24 Å^{-1}; Δr = 2.57 Å).

Temperature-Programmed Desorption

The profile for desorption of H_2 from the decarbonylated sample made from $[HIr_4(CO)_{11}]^-$ (Fig. 2) includes two small peaks, at 200 and 260°C, and larger peaks, at 400 and 440°C. The area of the latter two peaks is five times that of the former two.

Catalytic Hydrogenation of Cyclohexene

In a blank test, no cyclohexene conversion was observed at 25°C with the MgO support in the absence of iridium. When the MgO-supported catalysts were used in the reaction, cyclohexane was the only product detected by gas chromatography. In typical experiments, the reaction was allowed to proceed for 3–4 h, although in one experiment (with a conversion of 0.18%), data were collected for 15 h. In all the experiments, there was a linear dependence of conversion on time, indicating that the catalyst was stable, undergoing no measurable deactivation under these reaction conditions. The conversion data were used to calculate rates of the cyclohexene hydrogenation reaction for each catalyst sample. Figure 3 shows conversion vs time for the cyclohexene hydrogenation catalyzed by the sample made from $[HIr_4(CO)_{11}]^-$ on MgO. The slope is the reaction rate; rates are expressed as TOF, i.e., numbers of cyclohexene molecules transformed into product per Ir atom per second. The dispersion (fraction of iridium exposed) in the catalyst was taken to be 100% on the basis of the EXAFS results. TOF values were unaffected by changes in the stirring rate.

The TOF for cyclohexene hydrogenation was found to be 0.018 ± 0.006 s^{-1}, where the error bound represents the standard deviation based on six measurements, each made with a separately prepared catalyst sample. Thus the error bound indicates inconsistencies both in catalyst preparation and rate measurements.

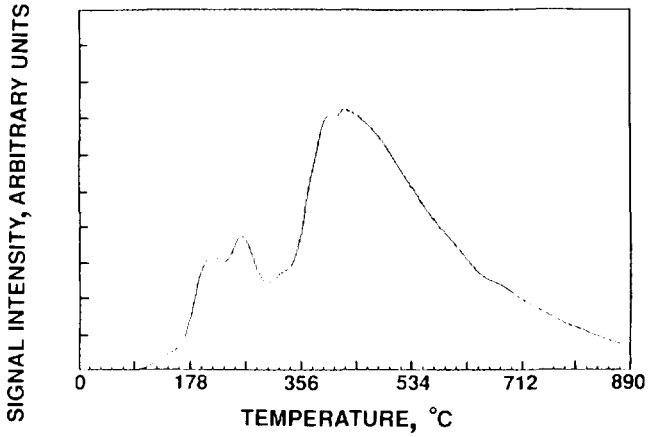

FIG. 2. Temperature-programmed desorption profile for hydrogen desorption from the sample made by decarbonylation of $[HIr_4(CO)_{11}]^-$ supported on MgO.

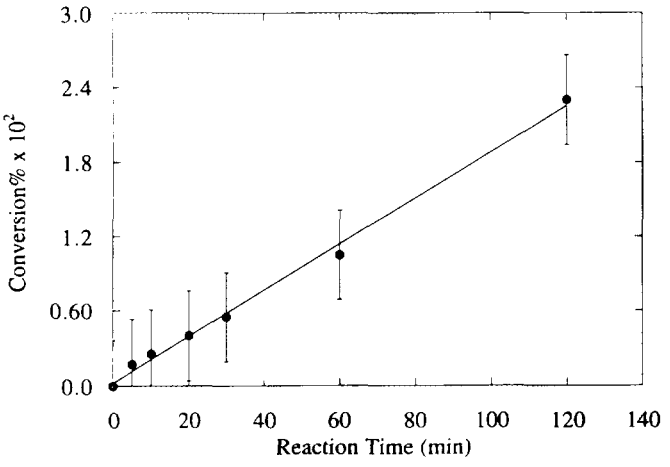

FIG. 3. Cyclohexene hydrogenation at 25°C catalyzed by MgO-supported clusters prepared by decarbonylation of $[HIr_4(CO)_{11}]^-$. The slope of the curve determines the rate of reaction. The error bars indicate the standard deviations in conversion determined in six experiments, each with a separately prepared catalyst sample.

The TOF measured for the AESAR $Pt/\gamma\text{-}Al_2O_3$ was estimated on the basis of the exposed Pt atoms, determined from the dispersion of 0.83. The TOF is 4.3 ± 0.9 s^{-1}. The value was repeated within ±10% for the Pt/Al_2O_3 sample with a dispersion of 0.65. For comparison, the TOF that is most nearly comparable to this value, as determined by Madon *et al.* (3), for 0.6 wt% platinum supported on $\gamma\text{-}Al_2O_3$ is 8.6 s^{-1}. Nearly the same results (TOFs in the range of 7.7 to 9.2 s^{-1}) were obtained by Madon *et al.* for platinum on SiO_2 and on other aluminas.

DISCUSSION

Advantages of Organometallic Precursors in Preparation of Structurally Simple Supported Metal Clusters

The supported metal clusters that can be characterized most precisely with EXAFS spectroscopy are those that are the smallest and most nearly uniform. A unique advantage of molecular metal carbonyl cluster precursors is the opportunity they offer for preparation of extremely small and nearly uniform supported metal clusters. The results presented here, consistent with earlier reports (12, 13), give evidence that the tetrairidium clusters can be decarbonylated on the MgO support with little if any change in nuclearity. Metal carbonyl precursors also offer the advantage of having no chloride or other components that would remain as catalyst poisons. Hence highly dispersed and, in prospect, nearly uniform supported metal clusters derived from organometallic precursors offer the opportunity for preparing structurally well-defined supported metal clusters that may allow experiments to show the dependence of catalytic properties on cluster nuclearity.

Structures of Clusters Formed by Decarbonylation of $[HIr_4(CO)_{11}]^-$ Supported on MgO

Van Zon *et al.* (12) and Kawi *et al.* (23) used EXAFS spectroscopy to characterize clusters formed by decarbonylation of $[HIr_4(CO)_{11}]^-$ on MgO. The former authors reported an Ir–Ir first-shell coordination number of 2.6 ± 0.3; the latter authors reported a value of 3.1, and the value determined in the research reported here for the used catalyst is 3.3. For comparison, the precursor $[HIr_4(CO)_{11}]^-$ has an Ir–Ir coordination number of 3.0 and a tetrahedral metal frame, as determined crystallographically for the $[NBu_4]$ salt of this anion (14). In view of the expected experimental error of about ±20%, the coordination number determined for the used catalyst by EXAFS spectroscopy is thus concluded to be indistinguishable from the values characteristic of the precursor and the other reported samples prepared from it. These results are all consistent with inference that the cluster nuclearity was maintained after decarbonylation and catalysis.

Van Zon *et al.* (12) modeled their supported clusters as a mixture of Ir_4 tetrahedra and square rafts, with about 40–50% of the clusters being tetrahedra. The results of Kawi *et al.* (23) and of the present research are suggestive of tetrahedral clusters, but they are not precise enough to rule out the presence of some similar structures in addition to tetrahedra. There were no Ir–Ir contributions observed at distances greater than that of the first Ir–Ir coordination shell in any of the cited work or in the work reported here, consistent with the absence of clusters larger than Ir_4. Thus, we refer to the clusters in the supported catalyst as Ir_4. There is a growing family of such supported clusters (24).

EXAFS Evidence of Stability of Supported Tetrairidium Catalyst

The EXAFS results characterizing the used catalyst demonstrated that the iridium clusters did not change substantially in structure during cyclohexene hydrogenation catalysis. The stability of the catalyst is also demonstrated by the near constancy of activity during operation. In the typical experiments, the reaction was carried out for 3 to 4 h. However, data were collected for 15 h in one experiment, and a straight line was obtained in the plot of conversion vs time, indicating that the catalyst underwent no measurable deactivation under these conditions. Thus the catalyst during operation is inferred to have consisted predominantly of Ir_4 tetrahedra supported on MgO. Because the MgO-supported iridium clusters had

been treated at 300°C in H_2 before the catalytic reaction, and because the reaction conditions were mild (25°C), it is not surprising that the framework structure of the cluster did not change significantly during catalysis.

The evidence of the stability of the catalyst and the reproducibility of the catalyst preparation and activity measurements, combined with the evidence that the clusters consisted predominantly of Ir_4, leads to the inference that the cyclohexene hydrogenation reaction was catalyzed by the Ir_4 clusters themselves. The inference that olefin hydrogenation is catalyzed by the metal clusters is consistent with the evidence that these clusters are catalytically active for toluene hydrogenation (25).

Comparison of Catalysis by Supported Ir_4 Clusters and Supported Metallic Clusters

The catalytic results characterizing the supported iridium clusters lend themselves to comparison with those reported by the Boudart group for various supported metallic catalysts. The reported results show (2, 8) that the rate of hydrogenation of cyclohexene catalyzed by metallic platinum does not depend significantly on the nature of the support or the average particle size of the metal. Approximately the same TOFs were found for the various noble metals (8). The fact that the TOF reported here for a supported platinum catalyst is approximately the same as these values confirms that the experimental procedures reported here nearly match those of Boudart *et al.* Because the reaction is first-order in hydrogen (3), the difference between the TOF for supported platinum reported here (4.3 s^{-1}) and that reported by Madon *et al.* (3) (8.6 s^{-1}) is attributed primarily to the fact that a lower hydrogen partial pressure was used in the present flow-reactor experiment (the H_2 partial pressure was not determined exactly) than in Madon's batch-reactor experiment. The possibility of a mass transport effect is not ruled out, but it is inferred that any such effect was small because of the near agreement of the rates observed with the Pt/γ-Al_2O_3 catalysts having different dispersions. Because the rate observed with the supported Ir_4 cluster catalyst was so much less than that observed with the supported Pt catalyst, it is inferred that mass transfer effects were negligible for the former.

Thus the striking result is the low value of the TOF for supported Ir_4 clusters relative to the values for the supported metallic catalysts. Consistent with this pattern, toluene hydrogenation rate data demonstrate that the activities of Ir_4 and Ir_6 clusters are markedly lower than that of highly dispersed metallic iridium on MgO (25). We conclude that the Ir_4 clusters are much less active than the metallic clusters and particles, both for cyclohexene hydrogenation and toluene hydrogenation.

Interaction of Hydrogen with Supported Iridium Clusters

The low activity of the Ir_4 clusters for cyclohexene hydrogenation corresponds to the low hydrogen chemisoption capacity of these clusters; the clusters adsorb only about a fourth as much hydrogen as metallic iridium. The TPD data, indicating that only a small amount of H_2 was desorbed at 200°C and a relatively large amount was desorbed at temperatures higher than 400°C, point to another contrast between the supported iridium clusters and conventional supported metallic catalysts. H_2 desorption from conventional supported metal catalysts has usually been observed at temperatures near or below 300°C (26, 27).

Aben *et al.* (26) reported the TPD of hydrogen from alumina-supported platinum catalysts that had been reduced at temperatures in the range 400 to 850°C to give samples with different metal particle sizes, which were estimated from H : Pt ratios determined in chemisorption experiments. The authors observed a small TPD peak at −20°C and two large overlapping peaks, one in the range 100 to 200°C and one in the range 200 to 300°C. The total amount of hydrogen adsorbed on the surface decreased as the average particle size increased; however, the peak indicating hydrogen that desorbed at −20°C remained virtually constant. The authors inferred that the metal–hydrogen interactions are stronger for small particles than for large ones. Aben *et al.* (26) also observed lower rates (TOFs) of benzene hydrogenation on their most highly dispersed catalysts than on the others.

Tsuchiya *et al.* (28) observed TPD peaks for hydrogen on platinum black at about −20, 90, and 300°C and tentatively assigned these peaks to Pt—H—H—Pt, Pt—H, and Pt—H—Pt, respectively, on the basis of the infrared spectra and theoretical calculations (29, 30).

Miller *et al.* (31) investigated the TPD of hydrogen from LTL zeolite-supported catalysts incorporating platinum clusters, estimated from EXAFS data to be 6 to 12 atoms in nuclearity. TPD of H_2 was performed after an initial reduction of the samples in H_2 at 300, 450, or 650°C. Reversible desorption of chemisorbed hydrogen occurred at approximately 175°C, and peaks corresponding to high-temperature irreversibly adsorbed hydrogen were observed at 300, 400, and 610°C. The TPD results reported here for Ir_4/MgO are similar to those reported by Miller *et al.* (31) for platinum clusters in zeolite LTL. The strength of the interaction may be related to the extreme smallness of the clusters.

The TPD peaks observed in the lower temperature range (100 to 200°C) are usually assigned to hydrogen chemisorbed on the metal, and one or more higher temperature peaks have been assigned by various authors to

spillover hydrogen (32–34), strongly chemisorbed hydrogen (35), hydrogen in subsurface layers of the metal (36), or oxidation of the reduced metal by support OH groups (37). The hypothesis of spillover hydrogen does not seem to be appropriate to explain the strong bonding of hydrogen to the small iridium clusters because the effect is not expected to be dependent on the metal cluster size. The EXAFS results indicate the presence of such small iridium clusters that subsurface layers were negligible; thus subsurface hydrogen is ruled out. Furthermore, if support OH groups had oxidized the metal during the treatment, the oxidation of the metal cluster would have been observed in the EXAFS data by the indication of a metal–oxygen distance of about 2.0 Å (21). The lack of an Ir–O interaction at such a distance (Table 1) suggests that there was negligible oxidation of the clusters. Therefore, we suggest that the high-temperature desorption peaks are evidence of hydrogen strongly chemisorbed on the iridium clusters and associated with their extreme smallness.

Limitation of the Concept of Structure Insensitivity

The low catalytic activity of Ir_4 relative to metallic catalysts correlates with the capacities of these structures for adsorption of H_2. Although the clusters catalyze the same reactions as metallic surfaces, their catalytic character is different. We infer that the clusters are metal-like but not metallic. The concept of structure insensitivity does not extend to clusters as small as Ir_4. The supported clusters are thus regarded as quasi-molecular, with the support providing part of a ligand shell, demonstrated by the EXAFS results (Table 1), which may affect the activity much as ligands affect the activities of molecular metal cluster catalysts.

CONCLUSIONS

MgO-supported $[HIr_4(CO)_{11}]^-$ was decarbonylated to form tetrairidium clusters on MgO, as shown by the results of infrared and EXAFS spectroscopies. The EXAFS results are consistent with the inference that the catalysts consisted of Ir_4 clusters on the support during and after catalysis of cyclohexene hydrogenation at 25°C. Hydrogen chemisorption and TPD results show that the extremely small metal clusters have properties distinct from those of supported metallic catalysts. Hydrogen interacts strongly with the iridium clusters, some being desorbed only at a high temperature (440°C). The turnover frequency for cyclohexene hydrogenation at 25°C and 1 atm was found to be $0.018 \pm 0.006\ s^{-1}$. This rate is two orders of magnitude less than that observed for a conventional highly dispersed supported platinum catalyst. These are the first results characterizing the catalytic performance of such small and structurally uniform supported metal clusters. The concept of structure insensitivity pertains to metallic particles larger than about 10 Å in diameter but does not extend to clusters as small as Ir_4, which are regarded as quasi-molecular and not metallic.

ACKNOWLEDGMENTS

This work was supported by the National Science foundation (grant CTS-9315340)

REFERENCES

1. Boudart, M., *Adv. Catal.* **20,** 153 (1969).
2. Boudart, M., and Djéga-Mariadassou, G., "Kinetics of Heterogeneous Catalytic Reactions." Princeton Univ. Press, Princeton, NJ, 1984.
3. Madon, R. J., O'Connell, J. P., and Boudart, M., *AIChE J.* **24,** 104 (1978).
4. Segal, E., Madon, R. J., and Boudart, M., *J. Catal.* **52,** 45 (1978).
5. O'Rear, D. J., Loffler, D. G., and Boudart, M., *J. Catal.* **94,** 225 (1985).
6. Leclercq, G., and Boudart, M., *J. Catal.* **71,** 127 (1981).
7. Gonzo, E. E., and Boudart, M. *J. Catal.* **52,** 462 (1978).
8. Boudart, M., and Sajkowski, D. J., *Trans. Faraday Soc.* **92,** 57 (1991).
9. Boudart, M., and McConica, C. M., *J. Catal.* **117,** 33 (1989).
10. Davis, S. M., and Somorjai, G. A., *J. Catal.* **65,** 78 (1980).
11. Schmid, G., Ed., "Clusters and Colloids." VCH, Weinheim, 1994.
12. Van Zon, F. B. M., Maloney, S. D., Gates, B. C., and Koningsberger, D. C., *J. Am. Chem. Soc.* **115,** 10317 (1993).
13. Maloney, S. D., van Zon, F. B. M., Koningsberger, D. C., and Gates, B. C., *Catala. Lett.* **5,** 161 (1990).
14. Bau, R., Chiang, M., Wei, C., Garlaschelli, L., Martinengo, S., and Koetzle, T., *Inorg. Chem.* **23,** 4758 (1984).
15. Vandenberg, D. M., Ph.D. dissertation, University of California, Santa Barbara, 1986.
16. Lin, S. D., and Vannice, M. A., *J. Catal.* **143,** 539 (1993).
17. Teo, B. K., and Lee, P. A., *J. Am. Chem. Soc.* **101,** 2815 (1979).
18. Van Zon, J. B. A. D., Koningsberger, D. C., van't Blik, H. F. J., and Sayers, D. E., *J. Chem. Phys.* **82,** 5742 (1985).
19. Kampers, F. W. H., and Koningsberger, D. C., *Faraday Disc. Chem. Soc.* **89,** 137 (1990).
20. Kirlin, P. S., van Zon, F. B. M., Koningsberger, D. C., and Gates, B. C., *J. Phys. Chem.* **94,** 8439 (1990).
21. Koningsberger, D. C., and Gates, B. C., *Catal. Lett.* **14,** 271 (1992).
22. Koningsberger, D. C., and Prins, R. "X-ray Absorption: Principles, Applications, Techniques of EXAFS, SEXAFS and XANES," p. 395. Wiley, New York, 1988.
23. Kawi, S., Chang, J.-R., and Gates, B. C., *J. Phys. Chem.* **98,** 12978 (1994).
24. Gates, B. C., *Chem. Rev.*, in press.
25. Xu, Z., Xiao, F. S., Purnell, S. K., Alexeev, O., Kawi, S., Deutsch, S. E., and Gates, B. C., *Nature (London)* **372,** 346 (1994).
26. Aben, P. C., Van Der Eijk, H., and Oelderik, J. M., "Proceedings, 5th International Congress on Catalysis 1972," p. 671.
27. Foger, K., and Anderson, J. R., *J. Catal.* **54,** 318 (1978).
28. Tsuchiya, S., Amenomiya, Y., and Cvetanovic, R. J., *J. Catal.* **19,** 245 (1970).

29. Szilagyi, T., *J. Catal.* **121,** 223 (1990).
30. Pliskin, W. A., and Eischens, R. P., *Z. Phys. Chem.* **24,** 11 (1960).
31. Miller, J. T., Meyers, B. L., Modica, F. S., Lane, G. S., Vaarkamp, M., and Koningsberger, D. C., *J. Catal.* **143,** 395 (1993).
32. Kramer, R., and Fischbacher, M., *J. Mol. Catal.* **51,** 247 (1989).
33. Dou, L. Q., Tan, Y. S., and Lu, D. S., *Appl. Catal.* **66,** 235 (1990).
34. Kramer, R., and Andre, M., *J. Catal.* **58,** 287 (1979).
35. Menon, P. G., and Froment, G. F., *J. Catal.* **59,** 138 (1979).
36. Levy, P. J., and Primet, M., *Appl. Catal.* **70,** 263 (1991).
37. Homeyer, S. T., Karpinski, Z., and Sachtler, W. M. H., *J. Catal.* **123,** 60 (1990).